AIAA JOURNAL
Vol. 46, No. 9, September 2008

Flapping-Wing Aerodynamics: Progress and Challenges

Max F. Platzer* and Kevin D. Jones†
Naval Postgraduate School, Monterey, California 93943
and
John Young‡ and Joseph C. S. Lai§
University of New South Wales at the Australian Defence Force Academy, Canberra, 2600, Australia

DOI: 10.2514/1.29263

It is the objective of this paper to review recent developments in the understanding and prediction of flapping-wing aerodynamics. To this end, several flapping-wing configurations are considered. First, the problem of single flapping wings is treated with special emphasis on the dependence of thrust, lift, and propulsive efficiency on flapping mode, amplitude, frequency, and wing shape. Second, the problem of hovering flight is studied for single flapping wings. Third, the aerodynamic phenomena and benefits produced by the flapping-wing interactions on tandem wings or biplane configurations are discussed. Such interactions occur on dragonflies or on a recently developed micro air vehicle. The currently available two- and three-dimensional inviscid and viscous flapping-wing flow solutions are presented. It is shown that the results are strongly dependent on flapping frequency, amplitude, and Reynolds number. These findings are substantiated by comparison with the available experimental data.

Nomenclature

A	=	wake width
a	=	plunge amplitude
b	=	span
c	=	chord
C_p	=	power coefficient, $P/(q_\infty c)$
C_t	=	thrust coefficient, $T/(q_\infty c)$
f	=	flapping frequency, Hz
h	=	nondimensional plunge amplitude, a/c
k	=	reduced frequency, $2\pi fc/U_\infty$
L	=	lift
N	=	normal force vector
P	=	power
q	=	dynamic pressure, $\frac{1}{2}\rho U^2$
Sr	=	Strouhal number, fA/U_∞
T	=	thrust
U	=	velocity
x, y	=	Cartesian coordinates
α	=	angle of attack
η	=	propulsive efficiency, $C_t/C_p = TU/P$
θ	=	dorsoventral stroke angle
ρ	=	density
$(\cdot)_{\text{eff}}$	=	effective value
$(\cdot)_\infty$	=	freestream value

I. Introduction

BIRDS, insects, fish, and cetaceans, such as whales and dolphins, have evolved and used flapping-wing systems for thrust and lift production for millions of years. An understanding of their underlying aero/hydrodynamics therefore is of fundamental interest in itself [1]. Recently, the development of micro air vehicles (MAVs) has stimulated additional interest in this subject. The Defense Advanced Research Projects Agency (DARPA) defined MAVs as flying vehicles having no dimension larger than 15 cm. Future MAVs or NAVs (nano air vehicles) may be as small as common insects.

There is therefore an increased need to understand the flapping-wing mechanisms used in nature and to adopt or modify them for the design of flapping-wing vehicles. To this end, it is necessary to provide the vehicle designer with the aerodynamic knowledge and prediction tools required to select the flapping mechanism most suitable for the chosen mission objectives.

There have been a number of recent reviews on various aspects of flapping wing and biomimetic foil propulsion [1–5]. A complete review of the aerodynamics of bird and insect wings is beyond the scope of this paper. Rather, it is our objective to review current knowledge of the physics of thrust and lift generation by means of wing flapping and to present the analysis methods and results that are currently available to determine the aerodynamic characteristics of single flapping airfoils or wings in cruise or hover flight as well as the benefits to be obtained by oscillating tandem or biplane airfoil or wing combinations. We limit ourselves to the discussion of the aerodynamics generated by the pitch and/or plunge motions of airfoils and finite-span wings or airfoil/wing combinations in forward flight or by their back and forth motion with rapid rotation at the end of the stroke in still air (hover mode). We use the term flapping for convenience to comprise any of these motions.

Critical similarity parameters for characterizing oscillatory flows (namely, the Strouhal number and reduced frequency), the Knoller–Betz effect that leads to thrust from oscillating wings, and various analysis methods are first briefly described. Reynolds number is also a critical parameter that influences flapping-wing flight. For example, in nature the flapping strategies used at higher Reynolds numbers by birds are very different from those used by most insects at lower Reynolds numbers in which massive leading-edge separation is common. Although we do not directly address these strategies, Reynolds number effects pertaining to leading-edge separation, vortex shedding, and aerodynamic performance as calculated by inviscid and viscous solvers are discussed in all subsequent sections. In Sec. II, the physics of thrust generation and propulsive efficiency of a pure plunging airfoil is examined using inviscid flow (both linearized potential flow and panel methods) and Navier–Stokes solvers complemented by experimental data. This analysis is then extended in Sec. III to single flapping airfoils which

Received 13 December 2006; revision received 16 August 2007; accepted for publication 5 November 2007.

*Distinguished Professor Emeritus of Mechanical and Astronautical Engineering. Fellow AIAA .
†Research Associate Professor of Mechanical and Astronautical Engineering. Senior Member AIAA.
‡Lecturer, School of Aerospace, Civil, and Mechanical Engineering. Member AIAA.
§Professor and Associate Dean (Research). Associate Fellow AIAA.

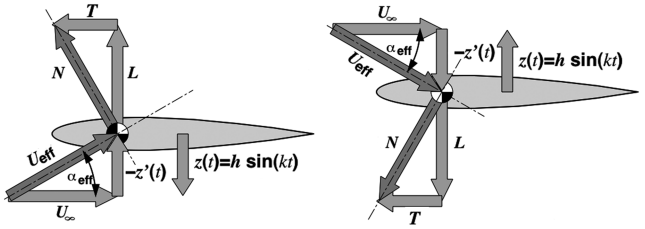

Fig. 1 First theory describing propulsion from flapping wings, Knoller [6] and Betz [7].

combine both pitching and plunging motions with elastic wing and three-dimensional effects being described. The physics of hovering flight is discussed in Sec. IV with reference to analytical, computational, and experimental data. In Sec. V, wing/vortex interactions in forward and hovering flight are examined and the development of a novel flapping-wing MAV based on the principles discussed here is illustrated. Finally, a summary of the state-of-the-art flapping-wing aerodynamics and challenges for future research is given in Sec. VI.

Knoller [6] and Betz [7] were the first to observe that a flapping wing creates an effective angle of attack so that an aerodynamic force, N, is generated which decomposes into lift and thrust components. This is illustrated in Fig. 1 in which the wing is shown during the downstroke and upstroke. A positive thrust component is generated during both strokes, yielding a time-averaged positive thrust as a result of wing flapping. Katzmayr [8] provided the first experimental verification of the Knoller–Betz effect when he placed a stationary wing into a sinusoidally oscillating wind stream and measured an average thrust.

Taylor et al. [9] analyzed the flapping frequencies and amplitudes of 42 species of birds, bats, and insects in cruise flight and found that these flying animals operate within a narrow range of Strouhal number between 0.2 and 0.4, in which the Strouhal number is defined as

$$Sr = fA/U_\infty \tag{1}$$

f being the flapping frequency in hertz, A the wake width, and U the flight speed. For flapping wings, A is usually taken as the length swept out by the wing tip. Taylor et al. [9] defined A as $b\sin(\theta/2)$ where θ is the dorsoventral stroke angle and b is the tip-to-tip wing span.

Their analysis shows that the dimensionless Strouhal number is a useful similarity parameter which appears to make it possible to characterize the flight performance of many flying animals ranging in size from small insects to albatrosses and kestrels. Its importance was already recognized by Birnbaum [10] who performed the first analysis of incompressible flow past oscillating airfoils using linearized potential flow theory. He called this parameter the reduced frequency.

At about the same time, Birnbaum [10] recognized that the Knoller–Betz model omitted an important part of the flow physics inherent in airfoil flapping, namely the shedding of starting vortices from the airfoil trailing edge. He showed that this problem was governed by the ratio of two characteristic speeds or characteristic lengths which led him to the introduction of a similarity parameter k, which is usually referred to as the reduced frequency, where

$$k = 2\pi fc/U_\infty \tag{2}$$

where f is the flapping frequency, c the airfoil chord, and U_∞ the flight speed. The product fc is a measure of the flapping velocity and hence k is a measure of the flapping velocity relative to the flight speed. Another interpretation of the reduced frequency is to regard it as the ratio of two characteristic lengths, namely the airfoil chord and the wavelength of the shed vorticity given by $U_\infty/2\pi f$. Another characteristic length is the flapping amplitude A. By using a nondimensional plunge amplitude, $h = a/c$, the relationship between the product kh and the Strouhal number Sr can be written as

$$kh = 2\pi(a/A)Sr \tag{3}$$

It should be noted that Eq. (3) relates a pure plunging motion to that of a general flapping motion. For a pure plunging motion that is uniform along the wing span, the ratio a/A is $1/2$ because the wake width is $2a$. However, for a flapping motion that is pivoted at one end as per birds and insects, the average length swept by a wing would be approximately half of that swept by the wing tip so that the ratio a/A is approximately $1/4$. Hence, Taylor's finding of an operating Strouhal number range of 0.2–0.4 is equivalent to a kh range of 0.3–0.6 for a pure plunging motion.

Still another interpretation of the kh value or of the Strouhal number is to remember that they indicate the angle of attack induced by the flapping motion, $\alpha_{\text{eff}} = \arctan(kh)$.

In 1935 von Kármán and Burgers [11] presented the first explanation of drag or thrust production based on the observed location and orientation of the wake vortices. At about the same time, Theodorsen achieved a solution for incompressible potential flow past oscillating airfoils valid for the complete reduced frequency range [12]. This allowed Garrick [13] to use this approach for the prediction of thrust and propulsive efficiency of harmonically plunging or pitching airfoils. As in Birnbaum's analysis, the assumption of small disturbance theory had to be made, thereby limiting the analysis to flat plates oscillating with small amplitude. This limitation could be removed with the availability of high-speed computers, making it possible to account for the effects of airfoil shape and amplitude whereas still retaining the potential flow assumption. Such approaches are based on the distribution of sources and vortices along the airfoil surface and are now generally referred to as panel methods. Unless otherwise stated the results shown in the present paper are based on a panel code developed by Teng [14]. Finally, over the past 20 years, it became feasible to drop the inviscid flow assumption and to achieve flow solutions based on the Navier–Stokes equations in which, for turbulent flow, the Reynolds averaging concept is being used in combination with a proper turbulence model. These three basic approaches, i.e., linearized, panel, and Navier–Stokes solutions, are described in more detail by Cebeci et al. [15]. We use them for the discussion of the aerodynamic characteristics of flapping wings. Contrasting the results of all three methods allows various aspects of the flow physics to be examined in detail.

II. Physics of Thrust Generation for Pure Plunge

For a first understanding of the physics of thrust generation it is instructive to observe the changes in vortex shedding from an airfoil which is oscillating in the pure plunge mode. In Fig. 2a the well-known Kármán vortex street is seen shed from a stationary NACA 0012 airfoil in a water flow of 0.2 m/s at a Reynolds number of about 17,000. As the airfoil starts to oscillate in plunge with increasing kh in Figs. 2b and 2c, the vortex wake is seen to transition until in Fig. 2d it is a *reverse* Kármán vortex street. This transition is seen to occur via the shedding of the vortex pairs shown in Figs. 2b and 2c. Note the product $kh = 2\pi Sr$. The upper row of vortices in the reverse Kármán vortex street has counterclockwise vortices, whereas the lower row has clockwise vortices. Obviously, flow is being entrained between these two vortex rows so that the time-averaged velocity distribution in planes perpendicular to the airfoil chord is that of a jet profile. The plunge oscillation therefore creates a jet and, as a reaction, a thrust on the airfoil. Jones et al. [16] measured the jet profile using laser-Doppler velocimetry and compared the measurements with the predictions using the above-mentioned panel code. An example of such a measurement is shown in Fig. 3. It is seen that the panel-code prediction is quite good. Therefore, the panel code was used for the prediction of airfoil thrust to determine its dependence on plunge frequency and amplitude. These computations are shown in Fig. 4 together with predictions by Garrick's linear theory and by Navier–Stokes computations. Thrust is seen to increase with increasing frequency and amplitude of oscillation. Of equal interest is the propulsive efficiency, which is defined as the ratio of thrust times flight velocity divided by the power required to

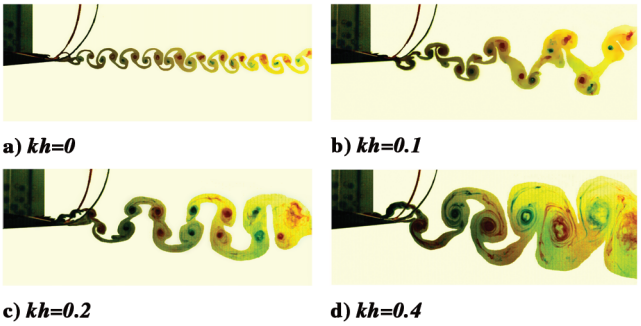

Fig. 2 Transition from normal to reverse Kármán vortex street with increasing *kh* [20].

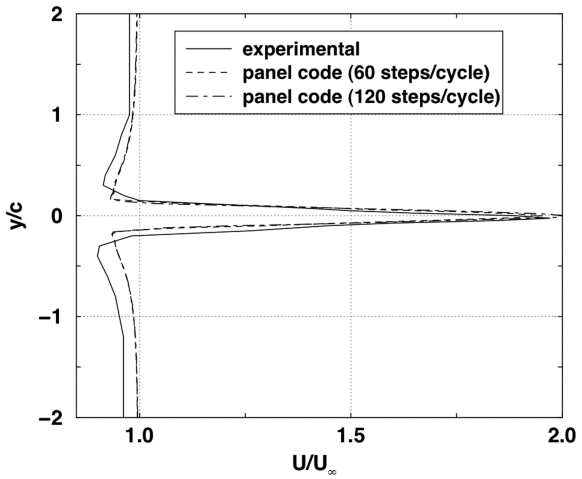

Fig. 3 Measured and predicted velocity downstream of a flapping wing ($kh = 0.6$).

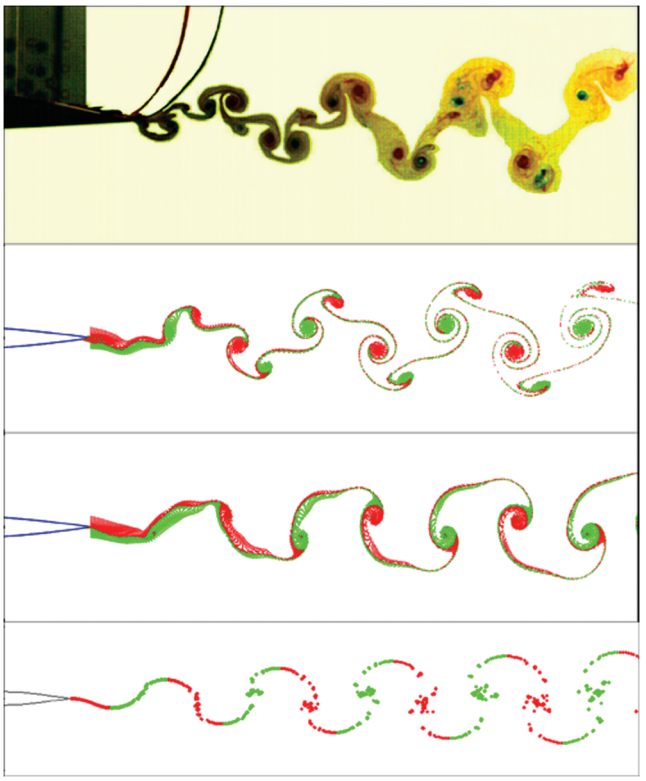

Fig. 5 Measured (upper frame) and predicted Navier–Stokes laminar and turbulent (second and third frames), and unsteady panel method (lower frame) vortex streets, $k = 8$, $h = 0.0125$ [18,24].

oscillate the airfoil. It might lead one to conclude that it is most efficient to flap a wing very slowly because the efficiency approaches unity as the reduced frequency approaches zero. However, because the thrust coefficient goes to zero with the reduced frequency, in a real flow, viscous and pressure drag quickly overtakes the small thrust generated, as seen in the Navier–Stokes results in Fig. 4. Further Navier–Stokes analyses of harmonically plunging airfoils were performed by Lewin and Haj-Hariri [17] and Young [18]. Note, panel code results are shown for both planar and deforming wakes in which the planar wake model emulates the wake of Garrick's linear theory, and the deforming wake allows shed vorticity to evolve over time. It is interesting to note that the planar wake model is virtually identical to linear theory, but the deforming wake solutions predict a higher thrust but lower efficiency.

Another look at Fig. 2 makes it clear that thrust production occurs only after a certain value of *kh* is exceeded because the transition from the drag-producing Kármán vortex street shed from the nonoscillating airfoil shown in Fig. 2a to the thrust-producing reverse Kármán vortex street occurs via the shedding of the vortex pairs in Fig. 2b. As shown by Young [18], the vortex-pair shedding requires a Navier–Stokes analysis. He analyzed a harmonically plunging NACA 0012 airfoil in a low-speed flow of Reynolds number 20,000. Young and Lai [19] pointed out that the vortex-pair shedding observed by Lai and Platzer [20] (Fig. 2b) is caused by the interaction between bluff-body type natural shedding from the trailing edge and the motion of the airfoil. They showed that there is a vortex lock-in region in the *k–h* plane in which this interaction can occur. They demonstrated that the separated flow behavior at and

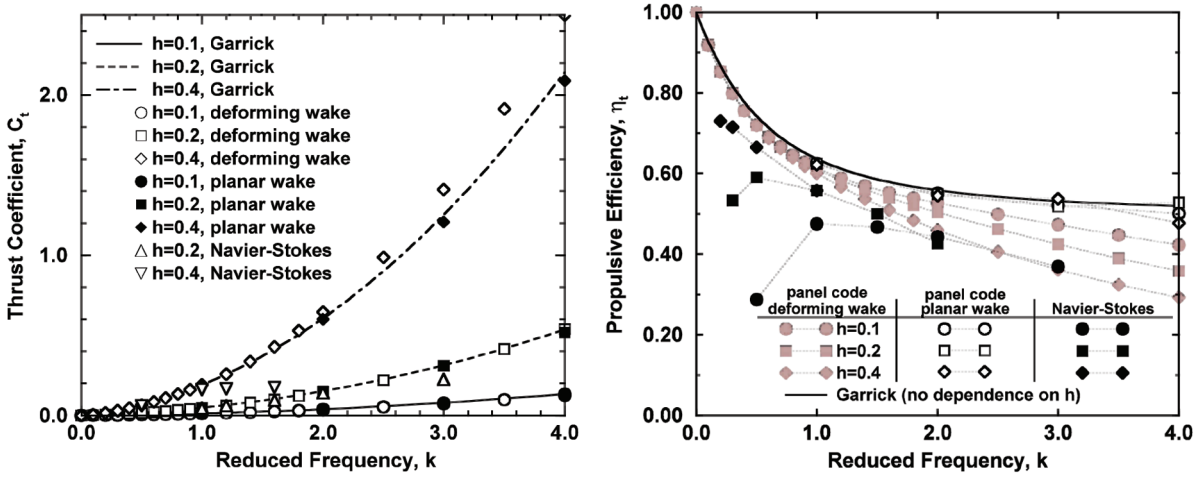

Fig. 4 Predicted thrust and efficiency as functions of frequency and amplitude.

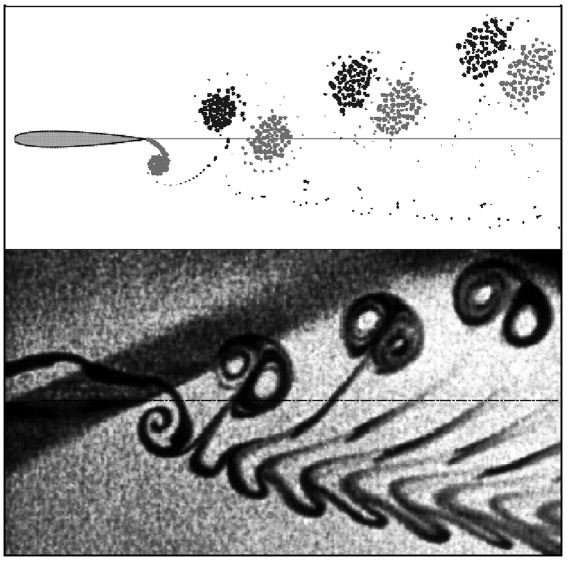

Fig. 6 Comparison of asymmetric vortex shedding [22], $kh = 1.5$ between panel-code prediction (upper frame) and flow visualization (lower frame).

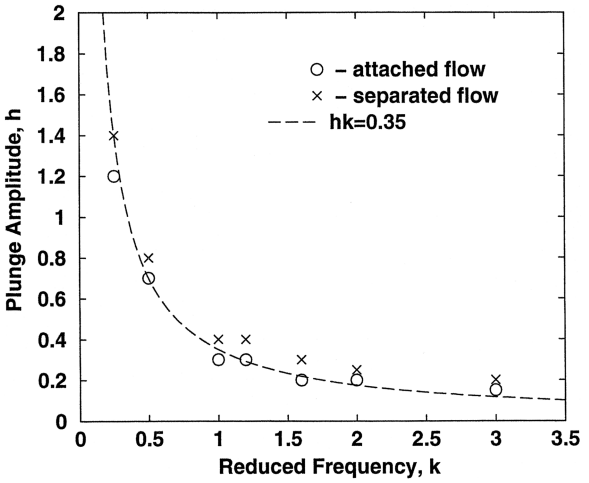

Fig. 7 Division of attached and separated flow in the h–k plane.

near the trailing edge becomes crucial in this region which, therefore, can only be predicted with a viscous flow analysis. Indeed, as seen in Fig. 5, they were able to reproduce the vortex patterns shown in Fig. 2b. Both laminar and turbulent (Baldwin–Lomax model) calculations are shown here. The turbulence model reduced the extent of the separation region near the trailing edge, reducing the strength of the bluff-body type shedding. An unsteady panel method calculation of the same case that eliminated the trailing edge separation region also completely eliminated the multiple-vortex-per-half-cycle wake structure.

Another type of vortex shedding occurs as the reduced frequency and the plunge amplitude are increased past certain critical values. Bratt [21] seems to have been the first one to observe the nonsymmetrical vortex shedding shown in Fig. 6, but he made no comment on these deflected vortex wakes. In fact, they were never again reported until 1998 when Jones et al. [22] studied them in greater detail both experimentally and computationally. They found that the deflected vortex street shown in Fig. 6 could be predicted with the panel code, suggesting that this type of vortex shedding is essentially an inviscid phenomenon. The cause seems to be the closeness of the shed vortices at high values of kh. However, because the product of amplitude and reduced frequency in this case was $kh = 1.5$, the maximum induced angle of attack therefore was about 56 deg, which is well above the dynamic stall limit for the airfoil. It is clear that at this high induced angle of attack there must be additional vortex shedding from the leading edge. Because an inviscid flow analysis cannot predict vortex shedding from the leading edge, a viscous flow computation is required to provide further flow details.

Tuncer et al. [23] performed Navier–Stokes computations of a sinusoidally plunging NACA 0012 airfoil in a flow of Mach number 0.3 at a Reynolds number of one million. They found that stall onset occurred at $kh = 0.35$ over a wide range of amplitude and reduced frequency values, as shown in Fig. 7. Thrust started to drop or, at the very least, to peak as soon as this dynamic stall boundary was crossed and the propulsive efficiency decreased quite dramatically. A kh value of 0.35 corresponds to a maximum induced angle of attack of about 19 deg. Hence, the loss of thrust and efficiency at flow conditions with dynamic stall is quite consistent with expectations.

However, Navier–Stokes computations by Young and Lai [24,25] for the same airfoil in incompressible flow in the Reynolds number range between 10,000 to 30,000 reveals significant differences compared with the high-Reynolds number behavior. Figure 8 shows the predicted propulsive efficiencies as a function of kh for three different nondimensional amplitudes and for three different reduced frequencies. Also shown is the comparison with the measured values of Heathcote et al. [26]. It is seen that the peak efficiency occurs at a kh value of approximately 0.4, except for the lowest frequency case. This indicates that a boundary exists similar to the dynamic stall boundary for high-Reynolds number flow beyond which there is a sharp drop in efficiency. However, at Reynolds numbers between 10,000 to 30,000 a kh value of 0.4 corresponds to a maximum induced angle of attack of 22 deg, which is far greater than the static stall angle in this Reynolds number range. Indeed, Figs. 9a and 9b show the shedding of vortices from the leading edge at the kh value for optimum efficiency both for low-amplitude and high-amplitude

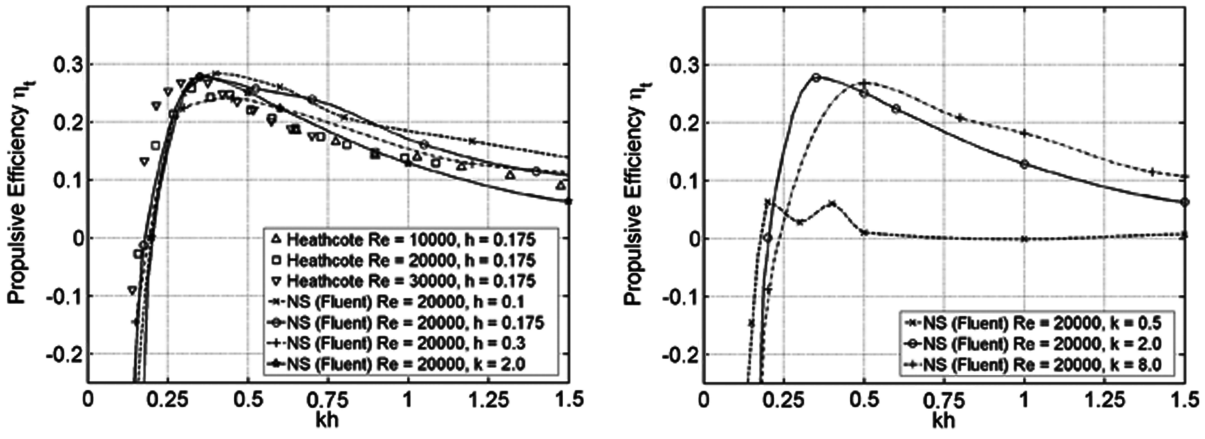

a) h = constant **b) k = constant**

Fig. 8 Propulsive efficiency of pure plunging at various amplitudes and frequencies.

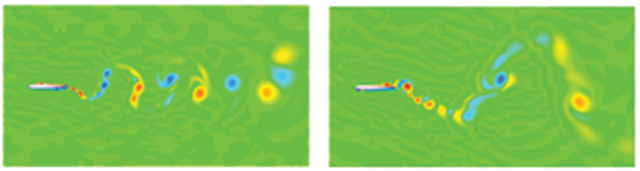

a) $k=4.0$, $h=0.1$ b) $k=1.5$, $h=0.3$

Fig. 9 Vorticity contours, pure plunging.

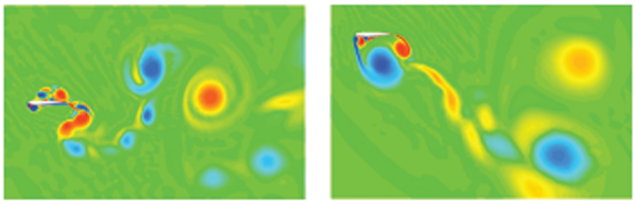

a) $k=2.0$, $h=0.75$ b) $k=0.5$, $h=3.0$

Fig. 11 Vorticity contours, pure plunging.

oscillation in plunge. Although leading-edge vortices are detrimental to the production of thrust at high-Reynolds numbers, their effect at low-Reynolds number flows is outweighed by the increase in strength of the trailing edge vortices so that the net thrust increases with kh even in the presence of leading-edge vortices. In Fig. 10 the computed thrust values are plotted as functions of reduced frequency and amplitude. The good agreement with experimental values lends credibility to the Navier–Stokes prediction. It is seen that thrust continues to increase with increasing kh values in spite of the shedding of strong leading-edge vortices. However the greatly reduced thrust at low k for a given kh value (such as 1.5) as depicted in Fig. 10b is due to massive leading-edge shedding as shown in Figs. 11a and 11b. Additional information on the aerodynamic forces generated by a plunging NACA 0012 airfoil has been published by Young and Lai [24,25].

These results indicate that the physics of thrust generation by an airfoil flapping in the pure plunge mode is strongly dependent on a number of parameters. At high-Reynolds numbers, efficient thrust generation is achieved by the shedding of trailing edge vortices in the form of the reverse Kármán vortex street that forms as soon as a sufficiently large Strouhal number is reached. Maximum thrust and optimum efficiency occur at operation near the dynamic stall boundary for a constant value of the Strouhal number. Hence, the Strouhal number is the major parameter that governs the flow behavior in this regime. However, at low-Reynolds numbers, typical for micro air vehicle flight, the flow behavior is much more complex because efficient thrust generation is achieved by shedding from both leading and trailing edges. Although the most efficient flight condition appears to occur again for a specific Strouhal number, thrust and propulsive efficiency are sensitive to the plunge frequency independent of Strouhal number due to the time for leading-edge vortex formation, separation, and convection over the airfoil surface. The results of Young and Lai [25] indicate that for a given kh (hence Strouhal number) it is more beneficial to operate at a high k and a low h than at a low k and a high h to minimize the adverse effect of the leading-edge vortex. These findings are largely based on computations and experiments for the NACA 0012 airfoil only.

Very recently, Lua et al. [27] investigated the wake structure generated by a harmonically plunging elliptic airfoil in a water flow of Reynolds number 1000. Using digital particle image velocimetry, they identified five different wake structures caused by different interactions between the vortices shed from the rounded leading and trailing edge dependent on frequency and amplitude.

III. Single Flapping Airfoils and Wings in Cruise Flight

Before drawing any further conclusions about the most efficient flapping flight mode it is necessary to consider other oscillation modes, namely pure pitching and combined pitch–plunge oscillation. Garrick [13] analyzed both the pure plunge and the pure pitch oscillation of a flat-plate airfoil in potential flow. He found that pure pitch oscillations start to generate thrust only after a relatively high frequency value has been exceeded. Koochesfahani [28] provided detailed flow visualizations and measurements. A comparison of linear and panel-code predictions with Koochesfahani's measurements is shown in Fig. 12, which confirms the unattractiveness of using pure pitch oscillations for thrust generation. Note that the predictions of linear theory and the panel code have been shifted by the $k=0$ drag measured by Koochesfahani (denoted as C_{do}).

Combined pitch–plunge oscillations, on the other hand, are a different matter. Indeed, virtually all examples of flapping-wing propulsion in nature combine pitching and plunging. The reason for the preference of combined pitch–plunge over pure-plunge oscillation can be deduced from Fig. 13 in which linear and panel-code analyses were performed for a NACA 0012 airfoil which pitched about its quarter chord point with an amplitude of 4 deg, whereas plunging with $k=0.5$ and $h=0.2$. Thrust, power, and efficiency are shown as a function of the phase angle between the pitch and plunge oscillation. The thrust coefficients are indicated by the light and dark solid lines (computed by linear theory denoted as "Garrick" and by the panel code, respectively). The power coefficients are indicated by the two dashed lines and the efficiencies by the two dash-dotted lines. Also note the two horizontal lines indicating the thrust coefficient and the efficiency for an airfoil executing a pure plunge oscillation. The efficiency is seen to reach

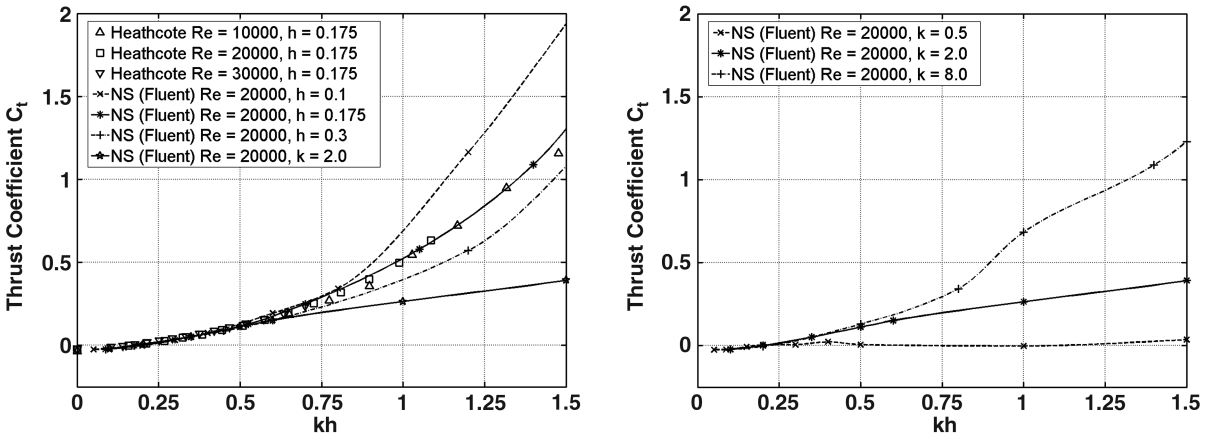

a) $h=$constant b) $k=$constant

Fig. 10 Mean thrust coefficient generated by pure plunging at various amplitudes and frequencies.

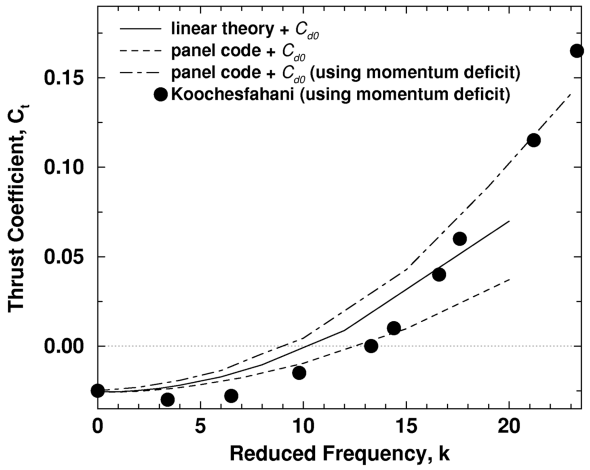

Fig. 12 Measured and predicted thrust coefficient for pitching airfoils [16].

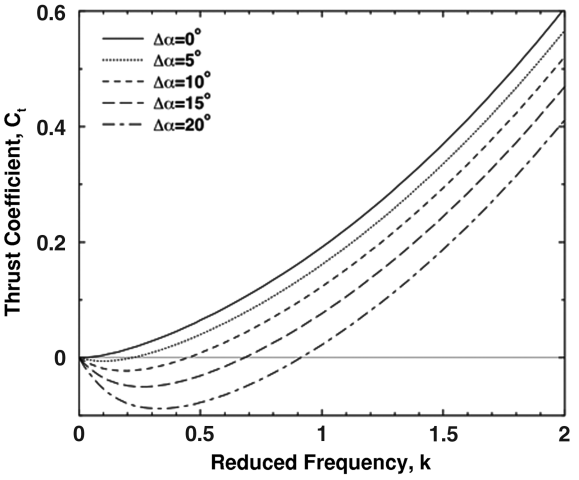

Fig. 14 Predicted thrust coefficient as a function of pitch amplitude $\Delta\alpha$ [16].

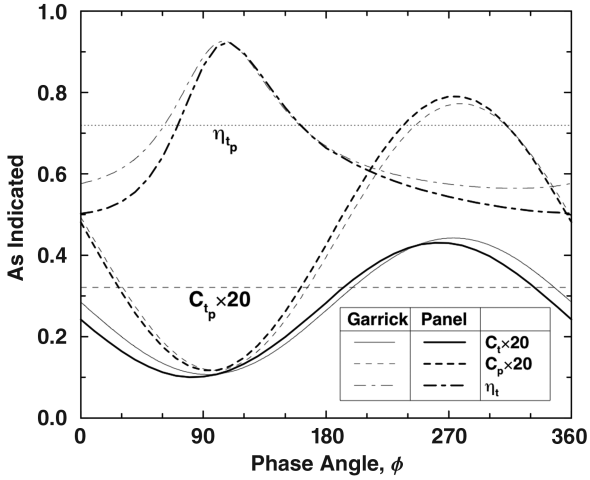

Fig. 13 Predicted performance for combined pitching/plunging motion [16].

rather high values when pitch leads plunge by about 90 deg. This is further substantiated in Fig. 14 in which the airfoil is flapped with the 90 deg phase angle. It is seen that the addition of a small amount of pitch amplitude $\Delta\alpha$ reduces the thrust generated by pure plunge only slightly.

Recently, Young and Lai [24] complemented the potential flow analysis of the NACA 0012 airfoil with Navier–Stokes computations and chose cases which were tested by Anderson et al. [29]. We show in Fig. 15 the case in which the plunge amplitude was 0.75, the pitch amplitude 15 deg, the pitch axis one-third chord, the phase angle between pitch and plunge 90 deg (pitch leading plunge) and the Reynolds number was 40,000. Shown are the thrust coefficient and the propulsive efficiency. It is seen that both the experiment and the Navier–Stokes calculations (laminar and turbulent) show a peak of the propulsive efficiency around a Strouhal number of 0.1–0.2. As the length scale used in the Strouhal number for these cases is dominated by the plunge amplitude, the most efficient Strouhal number range of 0.1–0.2 is approximately equivalent to the operating Strouhal number range of 0.2–0.4 found by Taylor et al. [9] for a flapping motion that is pivoted at one end, because in Taylor's case, the average length swept by a wing would be approximately half of that swept by the wing tip.

Further computations for the NACA 0012 airfoil in combined pitch–plunge oscillations were carried out by Isogai et al. [30] and Tuncer et al. [23] at a Reynolds number of 100,000. One example computation depicting the propulsive efficiency as a function of phase angle between pitch and plunge is shown in Fig. 16. It confirms the conclusion previously obtained with potential flow calculations that the optimum efficiency occurs when pitch leads plunge by about 90 deg. A closer inspection of the computed flowfields also shows that the efficiency drops rapidly in the presence of vortex shedding from the leading edge. This conclusion was further validated by Tuncer and Platzer [31]. Ramamurti and Sandberg [32] and Guglielmini and Blondeaux [33] studied the low-Reynolds number behavior by means of Navier–Stokes computations and a numerical solution of the vorticity equation, respectively. They obtained results at Reynolds numbers of 1100, which confirmed that optimum efficiency occurs at phase angles close to 90 deg and at Strouhal numbers between 0.125 and 0.2, consistent with the results shown in Fig. 15. But, as one would expect, the actual values are significantly lower than at the higher Reynolds numbers. Very recently, Young and Lai [25] discussed the mechanisms which influence the efficiency of oscillating airfoil propulsion. They presented Navier–Stokes computations for the NACA 0012 airfoil in combined pitch and plunge oscillation at Reynolds numbers between 20,000 and 40,000. Their results show that leading-edge vortex shedding and viscous drag decreases the propulsive efficiency quite substantially

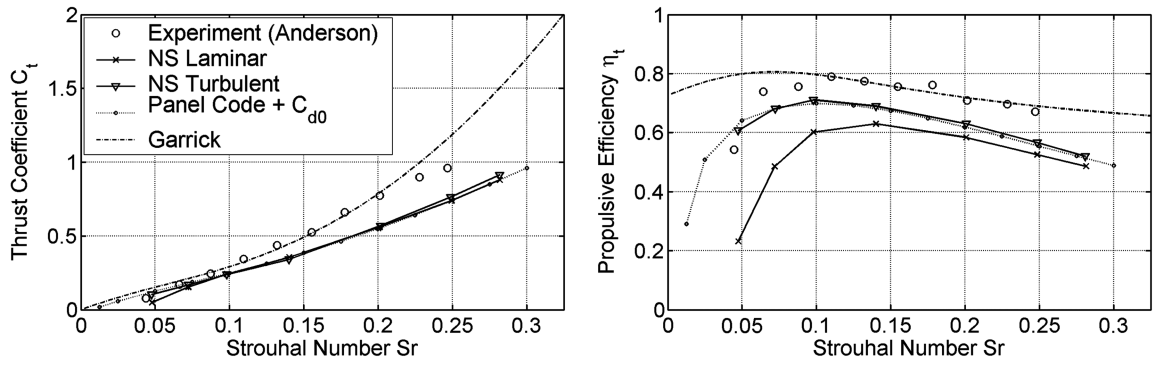

Fig. 15 Predicted and measured thrust and efficiency [25].

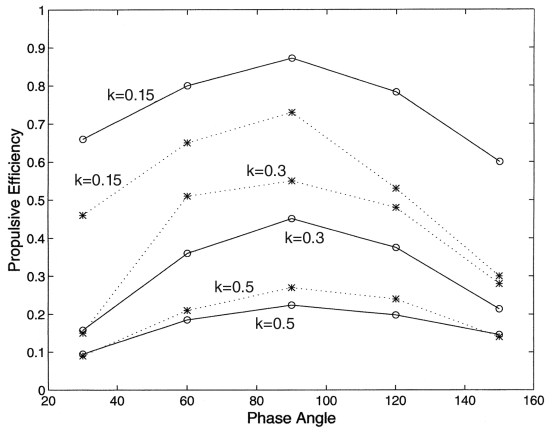

solid line: Tuncer et al. dotted line: Isogai et al.

Fig. 16 Propulsive efficiency as a function of frequency and phase [23].

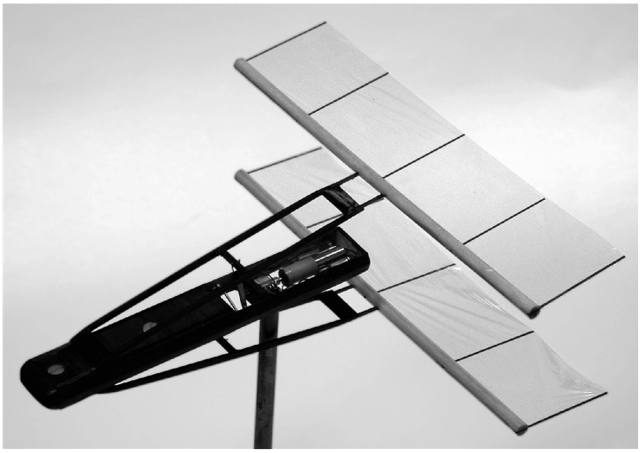

Fig. 17 Tuncer and Kaya MAV-sized propulsion test model [70].

at low Strouhal number and that the Strouhal number alone is insufficient to characterize the efficiency of flapping-foil propulsion.

Tuncer and Kaya [34] performed a systematic search for the optimum conditions by combining the Navier–Stokes code with an optimization procedure. They studied the NACA 0012 airfoil in a laminar flow of Reynolds number 10,000. Keeping the reduced frequency constant at $k = 1.0$ they searched for the pitch and plunge amplitudes and phasing between pitch and plunge which maximizes either the thrust or gives equal weighting to the thrust and the propulsive efficiency. They showed that at maximum thrust the airfoil sheds leading-edge vortices, whereas at combined maximum thrust and efficiency there is little shedding from the leading edge.

A. Elastic Wing Flapping

Although there is a growing interest in modeling and understanding the physics of flexible wing flapping, current development is largely restricted to employing membranes in fixed wings [2,35], and this field of study remains largely unexplored. Having shown in Fig. 16 that combined pitch–plunge oscillations are to be preferred over pure plunge oscillations for the attainment of good efficiency the question arises whether other oscillation modes can be used instead. To answer this question Heathcote and Gursul [36] performed water tunnel experiments on a harmonically plunging flexible airfoil with chordwise flexibility at Reynolds numbers between 9000 and 27,000. They found that an analogy can be made between a chordwise-flexible airfoil oscillating in plunge and a rigid airfoil oscillating in pitch and plunge in which the flexible airfoil offers the advantage of introducing pitch passively. They found that a degree of flexibility increases both thrust and propulsive efficiency. During the development of our flapping-wing MAV, we have also chosen to control only the plunge degree of freedom and to implement the pitch mode by supporting the wing elastically. The arrangement which we chose for thrust generation, i.e., two wings oscillating in counterphase, is shown in Fig. 17. Note that the two wings are attached to the flapping beams by means of flexible joints. We found that this way of introducing the pitch degree of freedom was crucial for the successful development of the MAV because a separate pitch control mechanism would have imposed too severe a weight penalty.

B. Three-Dimensional Flow Effects

In the preceding sections we limited the discussion to two-dimensional flows. For a more complete understanding of the physics of thrust generation by flapping wings it is necessary to account for finite-span effects. Fortunately, panel methods and, more recently, Euler and Navier–Stokes approaches have become available to provide information about the three-dimensional flow features generated by finite-span flapping wings. In Fig. 18, we show the flow downstream of a harmonically plunging finite-span wing which we computed using the CMARC panel code. It is seen that the

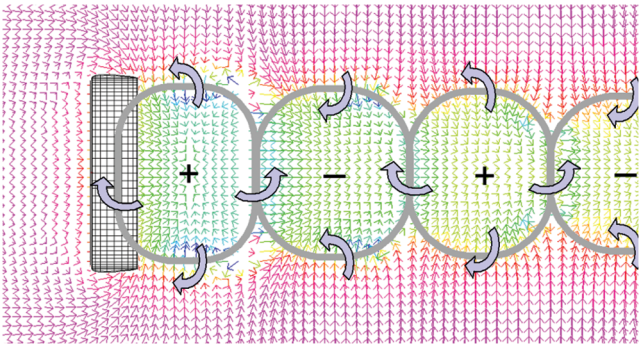

Fig. 18 Shed vorticity behind a finite-span flapping wing.

wing generates a series of vortex rings of alternating sign. A side view of the midspan flow would yield a reverse Kármán vortex street similar to that shown in Fig. 2d.

Neef and Hummel [37] studied the flow generated by a rectangular wing of aspect ratio eight with a NACA 0012 cross section that is flapping about its root section and pitching about the leading edge. They obtained Euler solutions for attached-flow conditions that provided details about the resulting unsteady trailing vortex system. Hall and Hall [38] also considered a root-based rectangular flapping wing. They used a vortex lattice method together with a variational method for computing the minimum power circulation distribution along the span of the flapping wing that must simultaneously generate thrust and lift. Both the induced power and the viscous profile power are minimized. This analysis showed that the optimal flapping frequency is one in which the wing flaps slightly less than once for every one wingspan the wing flies forward. Expressing this result in terms of the Strouhal number as defined by Eq. (1) values between 0.2 and 0.4 are obtained, thus again confirming the observation of Taylor et al. [9]. The three-dimensional flow structure behind a heaving and pitching finite-span wing in a flow of Reynolds number 164 was investigated by von Ellenrieder et al. [39] using dye flow visualization. They provided important information about the effect of Strouhal number, pitch amplitude, and phase angle between the pitch and plunge motion on the wake structure. Blondeaux et al. [40] performed a Navier–Stokes analysis of this experiment which confirmed the existence and shedding of the experimentally observed vortex rings. Using stereo multigrid digital particle image velocimetry Parker et al. [41] showed that the structure of the flow behind flapping wings with finite span is significantly more complex than the two-dimensional flow past flapping airfoils. This is due to the fact that the wing tip vortices significantly modify the wake flow. Very recently, Spentzos et al. [42] showed that the interaction between the 3-D dynamic stall vortex and the tip vortex is almost universal regardless of the planform shapes investigated.

IV. Hovering

A first insight into the flow physics of hovering flight can be gained by considering pure plunge oscillations of an airfoil in still air. An elliptic airfoil generates zero time-averaged thrust due to the symmetry of the resulting flow, as shown by Guglielmini and Blondeaux [33]. However, an airfoil with a rounded leading edge and a sharp trailing edge generates a finite thrust due to the vortex shedding from the trailing edge, as visualized by Lai and Platzer [43]. It stands to reason that in this case there is also shedding from the leading edge, but definitive visualization is still lacking. Heathcote et al. [44] made particle image velocimetry and force measurements of rigid and flexible airfoils, which showed the dependence of the shed vortices and of the thrust on the airfoil flexibility, plunge frequency, and amplitude. Freymuth [45] performed experiments that visualized the flow generated by an airfoil in combined harmonic plunging and pitching motion in still air. He investigated three different hovering modes that revealed strong vortices shed from both edges that organize efficiently into a jet structure and hence produce a large thrust. More recently, Sunada et al. [46] used a load cell with strain gages to measure the instantaneous forces acting on a wing undergoing a combined pitch–plunge motion and determined the combinations of these forces for maximum time-averaged thrust and for maximum efficiency. The experimental studies conducted by Ellington and Usherwood [47], Dickinson and Goetz [48], and others also revealed the crucial role of vortices shed from the leading edge to achieve the high lift values necessary for hovering.

Hummingbirds and many insects achieve hover with fully extended wings by moving the wings in an approximately horizontal plane. Although this wing motion occurs more in a figure eight type, it is sufficiently accurate to approximate the figure eight by two linear motions and two wing rotations at the stroke ends. These motions are shown in detail in Fig. 19. The airfoil is seen to *move to the left*, maintaining constant *positive* incidence and velocity, followed by a rotation around a point on the chord line so that the leading edge starts to point in the opposite direction, proceeding with constant incidence and velocity *to the right*, and rotating back at the end of the half-stroke *to the left*. As a result, the leading edge remains the leading edge during all four phases of the motion, but the upper and lower airfoil surfaces change roles from suction to pressure surface and vice versa. It is immediately apparent that the rotation to an incidence angle up to and past 90 deg causes the shedding of leading-edge vortices in addition to the shedding of starting and stopping vortices from the trailing edges as the airfoil decelerates to zero velocity and accelerates again.

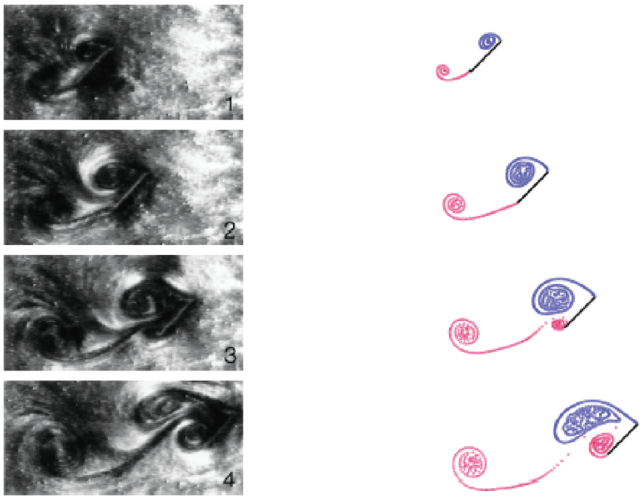

Fig. 20 Comparison of experimental [48] and numerical [52] results.

Dickinson and Goetz [48], Dickinson [49], and Sane and Dickinson [50] performed experiments which yielded quantitative aerodynamic force data for this type of motion. Their prediction, however, presents great challenges because of the vortex shedding and interaction processes which occur during this type of hovering motion. Zbikowski [51] and Ansari et al. [52] attacked this flow problem using potential flow modeling. An example of their analysis is shown in Fig. 20. It is seen that the vortex shedding from the leading and trailing edges compares well with the flow visualizations of Dickinson and Goetz [48].

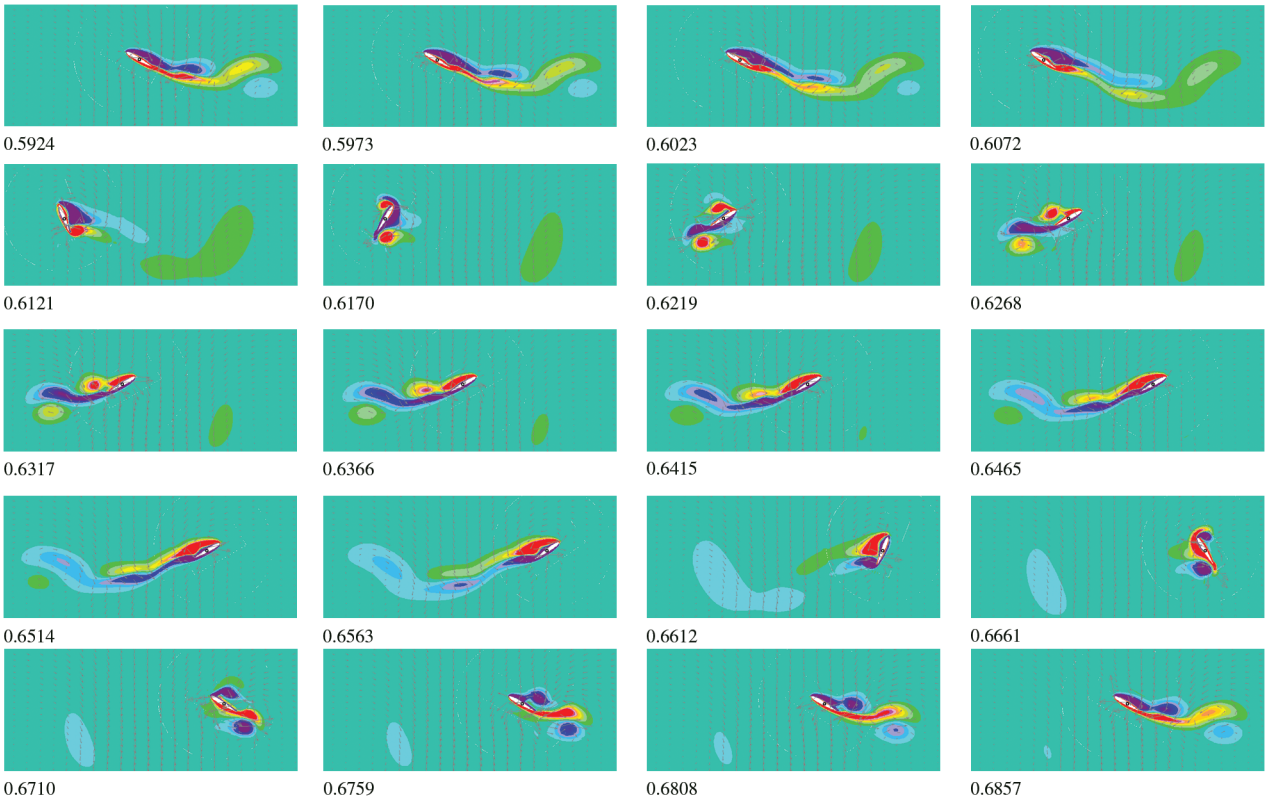

Fig. 19 Vorticity contours with velocity vectors for $\alpha = 30\,\mathrm{deg}, x_v = 2c, x_a = 2c, Re = 1000$ with rotation axis at $c/2$ during 7th stroke. Each frame is $(0.002 * T)$ second apart and the numbers in the lower left-hand corners represent the time in second (from [53]).

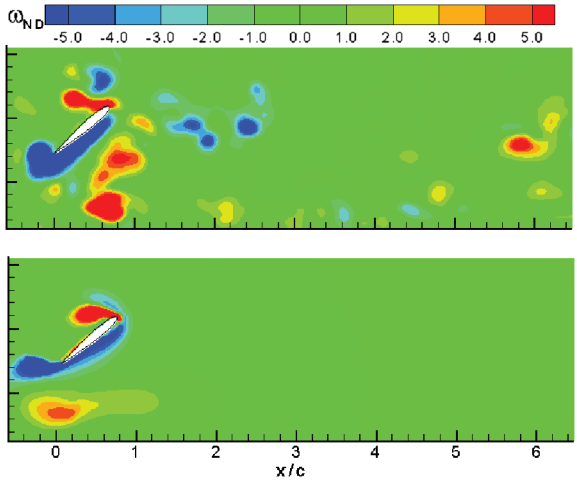

Fig. 21 Comparison between measured and computed vorticity fields [54].

Quite recently, Kurtulus et al. [53] applied laminar two-dimensional Navier–Stokes calculations that yielded detailed information about the vortex shedding and the effect of various parameters, such as airfoil incidence during the linear motions, location of start of incidence change, location of start of velocity change, location of pitch axis, and Reynolds number. A typical sequence of the computed vortex shedding during one stroke is shown in Fig. 21. Kurtulus et al. [54] also performed laser sheet visualization and particle image velocimetry measurements of this motion. An example of the comparison between the computations and the measurements is shown in Fig. 21.

Ellington and Usherwood [47] drew attention to the shortcomings of two-dimensional models to understand the physics of lift generation used by hovering insects. Instead, a better model might be the well-known conical vortices that form off the leading edges of delta wings at high angle of attack. On the hawk moth they discovered the formation of spiral leading-edge vortices due to strong spanwise flow in these vortices. The spanwise flow stabilizes the leading-edge vortex, thus prolonging the dynamic stall benefits for lift generation. This type of flow could indeed be reproduced using a three-dimensional Navier–Stokes computation per Liu et al. [55], Liu and Kawachi [56], and Liu [57]. Another three-dimensional Navier–Stokes computation for a hovering insect wing was recently performed by Ramamurti and Sandberg [58]. They studied the flapping wing of the fruit fly (*Drosophila*) and achieved good agreement with force measurements on a mechanical model built by Dickinson et al. [59]. Young et al. [60] investigated the effect of flapping amplitude, flapping frequency, and wing rotation timing and duration on the aerodynamic performance of the dragonfly hind wing using a three-dimensional Navier–Stokes solver. They found that the mean vertical force and power are essentially independent of frequencies exceeding 5 Hz and that the hovering efficiency peaks at a flapping amplitude of about 35 deg, very close to the observed amplitude of the dragonfly hind wing in hover.

V. Wing/Vortex Interactions in Forward and Hovering Flight

The foregoing discussion was limited to the consideration of single *airfoils* or wings that could oscillate either in a single mode (plunge or pitch), in a combined pitch–plunge mode, or in an aeroelastic mode. The resulting aerodynamics were seen to remain relatively simple as long as the flow over the wing stays attached because vortices are being shed only from the wing's trailing edge. However, the discussion of wings in hovering flight revealed the fact that vortex shedding from both leading and trailing edges is the key to effective lift generation in this flight mode. The understanding and prediction of the interaction between leading and trailing edge vortices therefore becomes essential.

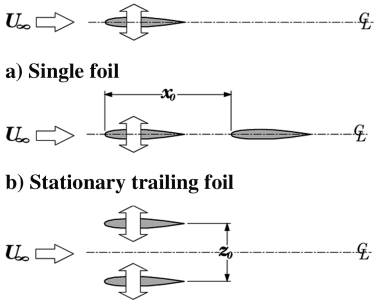

Fig. 22 Single and multiple airfoil schematics.

An even more complex interaction problem occurs when two flapping wings are arranged in close proximity to each other. The most common configuration is the tandem wing used by the dragonfly, although millions of years ago some insects seem to have also evolved the biplane configuration. Wootton and Kukalova-Peck [61] stated that the Homoiopteridae were an ancient group of large, sometimes gigantic insects that had forewings and hind wings which overlapped extensively. The same seems to have been the case for some members of the family Lycocercidae. No such overlapping is found on modern insects, leading to the interesting question for the reason for the disappearance of biplane insects (probably not good for hover mode).

Clearly, the fundamental challenge arises to study the aerodynamic interactions between two closely coupled wings that are arranged either in a tandem or biplane configuration and in which one or both wings are flapping. This situation seems to have been studied first by Bosch [62] using inviscid incompressible two-dimensional small disturbance flow theory. Bosch investigated the flow over two flat plates arranged in tandem. Each plate could oscillate either in pitch or plunge. He examined all possible combinations in which either the forward or the rearward plate is oscillating in pitch or plunge or both plates are oscillating. He found that a nonoscillating forward plate makes a negligible contribution to the total thrust of the tandem configuration, whereas a nonoscillating rearward plate significantly increases the thrust generated by a plunging forward plate. Furthermore, the propulsive efficiency of such a configuration is close to 100% and is nearly independent of the reduced frequency. Lan [63] analyzed the interaction between two finite-span wings by means of an unsteady quasivortex-lattice method and applied it to the study of dragonfly aerodynamics. He found that the tandem wings of the dragonfly can produce high thrust with high efficiency if the pitching is in advance of the plunging and the hind wing leads the fore wing with some optimum phase angle because the hind wing extracts wake energy from the fore wing.

The thrust and efficiency benefits that can be obtained from the placement of a nonoscillating airfoil behind but close to a plunging airfoil can be understood by recalling Katzmayr's [8] original experiment in which he measured a thrust force by placing a stationary airfoil into an oscillatory wind stream. In the tandem configuration with oscillating forward and stationary rearward airfoil, shown in Fig. 22b, the forward foil generates an oscillatory flow and which results in thrust generation by the rearward foil. In other words, the energy carried away in the vortices created by the forward foil is being converted into thrust instead of being swept away with the flow. This phenomenon was clearly recognized during the 1940s by Schmidt [64]. It inspired him to develop the configuration shown in Fig. 22b, which he called a *wave propeller*. He demonstrated the practical utility of his wave propeller on small catamaran boats and cited as a major advantage over conventional propellers its ability to operate in shallow waters although maintaining competitive efficiencies.

Because of these potential benefits Platzer et al. [65] and Tuncer and Platzer [66] analyzed this tandem configuration using panel and Navier–Stokes codes. These analyses confirmed the superiority of the tandem configuration over the single airfoil, but they also

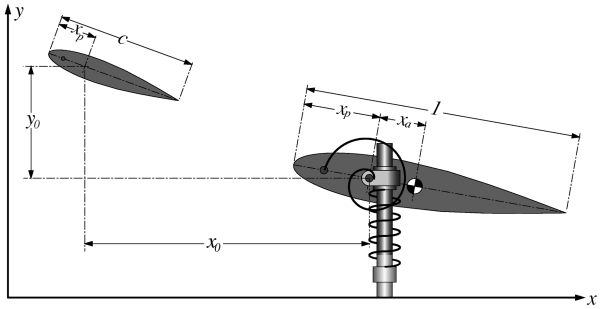

Fig. 23 Schematic of tandem, elastic airfoil experiment.

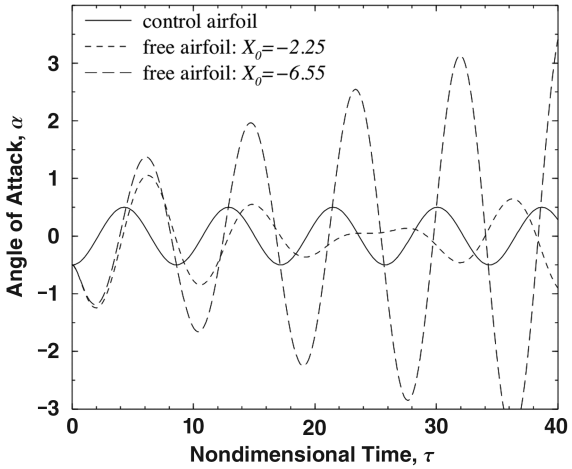

Fig. 24 Time history of pitch oscillations of the control and free wings.

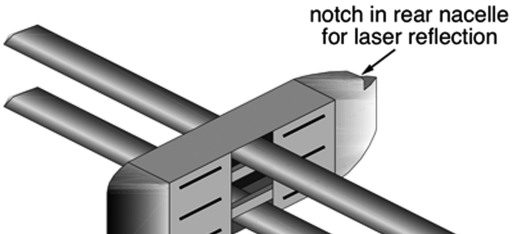

Fig. 25 Schematic of the biplane flapping mechanism.

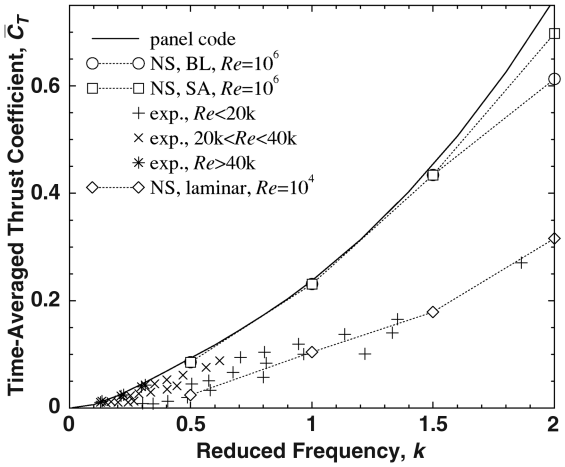

Fig. 26 Predicted and measured thrust.

revealed that viscous flow effects start to dominate at low reduced frequencies.

The effect of vortices shed from an upstream airfoil on a downstream airfoil can be demonstrated quite powerfully if the downstream airfoil is mounted on springs that allow it to oscillate both in pitch and plunge, as shown in Fig. 23. Jones and Platzer [67] analyzed this case with the panel code. As is well-known, an airfoil having the pitch and plunge degrees of freedom can easily encounter catastrophic flutter for certain combinations of the spring stiffnesses, elastic axis, and center-of-gravity positions. However, flutter can be suppressed by the shedding of vortices from a small upstream airfoil if the proper phasing of the vortex shedding is imposed. This is shown in Fig. 24.

The beneficial effect of vortex shedding from an upstream body was also noted by Zhu et al. [68]. They investigated the effect of vortices created on fish bodies in front of the fish tail on the swimming performance. Body-generated vortices can be repositioned and then paired with tail-generated same-sign vortices in such a way that a strong reverse Kármán vortex street and hence an increased thrust force is generated. On the other hand, destructive interference can also occur if the body-generated vortices are repositioned and then paired with tail-generated opposite-sign vortices in such a way that they weaken the reverse Kármán vortex street. This phenomenon therefore is quite similar to the above-mentioned phasing of the oncoming vortices to suppress or enhance flutter.

Another interesting interaction problem occurs in the biplane arrangement. Here the second airfoil is positioned opposite the first airfoil as its mirror image, as shown in Figs. 22c and 25. This arrangement emulates flow over a single airfoil in ground effect. If the airfoils flap in counterphase, symmetry is preserved, and the airflow should be equivalent to a single wing in ground effect.

Jones et al. [16] analyzed the biplane configuration using both panel and Navier–Stokes codes. In Fig. 26 the Navier–Stokes predictions are compared to the panel-code result and with thrust measurements of Jones et al. [69]. The high-Reynolds number turbulent flow predictions agree quite well with the inviscid panel-code results, but the predicted thrust drops dramatically for the low-Reynolds number, laminar flow computations. The experimental results are bracketed pretty well between the high- and low-Reynolds number predictions, with a clear trend as the Reynolds number is decreased. This strong Reynolds number dependency becomes understandable by examining the flowfield calculations that show virtually no flow separation on the two airfoils at the high-Reynolds number in contrast to the low-Reynolds number computation. Additional detailed Navier–Stokes calculations of a NACA 0014 biplane configuration at a Reynolds number of 10,000 were performed by Tuncer and Kaya [70]. Combined pitch and plunge oscillations produced 20–40% more thrust than a single airfoil.

The superiority of the biplane configuration over the tandem or the single wing arrangement motivated Jones et al. [71] to choose the micro air vehicle design shown in Fig. 27. Thrust is provided by the flapping wings in biplane arrangement, mounted in close proximity to the stationary wing that provides the required lift. This arrangement would appear to contradict Bosch's analysis showing that a stationary airfoil in front of an oscillating one is virtually unaffected by the presence of the oscillating airfoil. However, this conclusion holds only in inviscid flow. The entrainment effect caused by the oscillating airfoils turns out to be sufficiently strong to prevent boundary layer separation on the stationary wing, making this MAV design surprisingly gust insensitive and stall resistant. These design and flight performance aspects are discussed in more detail by Jones et al. [71].

We therefore turn now to the third interesting configuration in which the two wings are arranged in tandem, but both wings are flapping. It is the configuration used by dragonflies, among other insects. An overview of the kinematics and aerodynamics of the dragonfly was first given by Norberg [72]. This study was followed by several experiments conducted by Saharon and Luttges [73–75]

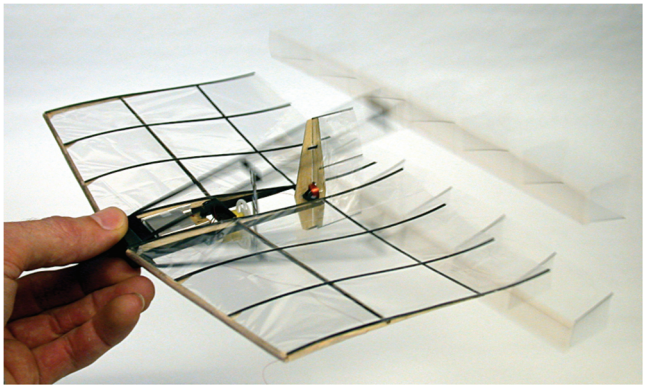

Fig. 27 Flapping-wing radio controlled MAV.

who visualized and analyzed the vortices shed from the two wings and their interactions with each other and with the neighboring wing. They observed that well-organized dynamic stall vortices are shed and that phase angle changes between the wing motions change the vortex interactions and in doing so control thrust and lift production. They concluded that the wing-vortex interactions generated by the dragonfly are a practical means to trap free vortices to enhance lift.

Given the complexity of these wing-vortex interactions it is not surprising that only a few computational analyses have been attempted. Lan [63] applied the doublet lattice method to obtain potential flow solutions for rectangular or arrow tandem wing configurations in forward flight in which both wings are flapping in a combined heave and pitch motion. He showed that it is advantageous to have both tandem wings oscillating, but with such a phase angle that the hind wing moves in advance of the fore wing.

Isogai and Shinmoto [76] analyzed the hovering flight of a tandem airfoil configuration. They used a Navier–Stokes code and confirmed the observations of Saharon and Luttges [73] that mutual interaction is crucial in generating the lift required to balance the body weight. Kim and Choi [77] performed a similar analysis and showed that the maximum lift force in hover was generated when the fore and hind wings were flapping with zero phase difference. Most recently, Isogai et al. [78] complemented their analysis with three-dimensional Navier–Stokes computations confirming that maximum hover lift is generated at zero phasing between the two wings. They also built a hovering robot that simulated the tandem wing interactions and found good agreement between the measured and computed lift values. Another hovering vehicle, the Mentor, was built at the Stanford Research Institute in California, in collaboration with the University of Toronto [79]. It exploits the Weis–Fogh or *clap-and-fling* effect, whereby two wings clap together and fling open in analogy to butterfly wings. Finally, we also mention that a very interesting micro air vehicle configuration, called the BITE vehicle, was developed at the Naval Research Laboratory. It adopts both the biplane and the tandem configuration and even uses wings with flexible camber. The name BITE stands for biplane insectoid travel engine. Ramamurti et al. [80] recently published a Navier–Stokes analysis of this unconventional air vehicle configuration.

VI. Summary

The primary interest in flapping-wing aerodynamics is in the determination of optimal lift, thrust, and efficiency. It has been recognized for many years that lift can be predicted remarkably well by an inviscid flow analysis provided the wing's Reynolds number is sufficiently large and the angle of attack is kept small. This simplification is made possible by the fact that the aerodynamic force normal to the freestream direction is little affected by the presence of the thin viscous boundary layer at high-Reynolds numbers. It is even possible to analyze wing flutter using inviscid flow methods because only the normal forces have an effect on flutter. Therefore, an extensive theory exists for the analysis of the flow over oscillating airfoils and wings.

In steady-state aerodynamics, the streamwise force, that is the drag force, can only be determined by the use of a viscous flow analysis to overcome d'Alembert's paradox. As interest in the aerodynamics of flapping wings increased in recent years, the question therefore arose whether the same reasoning applies to the prediction of the thrust force, thus necessitating viscous flow methods. The information presented in the preceding sections shows that inviscid flow methods retain considerable value because of their ability to provide quick predictions of thrust and propulsive efficiency as a function of important parameters, such as Strouhal number or phase angle between the pitch and plunge motions, as shown for example, in Figs. 4 and 13. It is also seen that the panel-code yields considerable improvements over linearized small-amplitude flat-plate theory. The good agreement between the measured and the panel-code predicted velocity distribution downstream of the harmonically plunging trailing airfoil trailing edge, shown in Fig. 3, indicates that the reverse Kármán vortex street is an essentially inviscid flow phenomenon. However, the available computational and experimental results also show the limitations of inviscid flow analyses and the strong dependence on Reynolds number. Viscous flow effects start to dominate for decreasing flow unsteadiness. As shown in Fig. 4, the inviscid flow predictions of the propulsive efficiency are quite optimistic at low Strouhal numbers, whereas the Navier–Stokes values are much reduced. As one would expect, the viscous effects become stronger with decreasing Reynolds number. This trend is clearly shown in Fig. 26, in which the measured thrust values are seen to decrease with Reynolds number. The available Navier–Stokes analyses confirm the strong dependence on Reynolds number. At a Reynolds number of one million, the shedding of leading-edge vortices occurs as soon as a critical Strouhal number is exceeded, as shown in Fig. 7, causing a rapid drop in thrust. In the low-Reynolds number range between 10,000 to 30,000, on the other hand, vortex shedding from the leading edge can be beneficial, as discussed with reference to Figs. 8–11.

Hence, significant progress has been made in the understanding of the major aerodynamic characteristics of flapping airfoils and airfoil combinations because of the ability to analyze two-dimensional unsteady airfoil flows with both inviscid and viscous flow codes and the acquisition of flow and force data. The aerodynamics of flapping airfoils in hovering flight is much less explored, although inviscid and viscous flow solutions have been developed in recent years and flow and force data have been acquired. As one would expect, the information available on the three-dimensional flow features of single and interacting flapping wings in forward or hovering flights is still quite limited.

NATO-RTO has responded to the need for research on low-Reynolds number aerodynamics and we refer to a recently issued report [81] for a review of progress in this field. The following challenges remain for a more complete understanding of flapping airfoil and wing aerodynamics:

1) Most flapping airfoil propulsion analyses and experiments have been limited to NACA, or to a lesser extent, elliptical airfoils. The effect of airfoil geometry, especially leading-edge geometry, remains to be systematically explored. Of particular importance is the physics governing the onset of vortex shedding from the leading edge and their interaction with the trailing edge vortices. Significant differences in flow behavior, especially with regard to onset of flow separation and vortex shedding from the leading edge have already been identified at low versus high-Reynolds numbers, but much more experimental information is needed to evaluate the adequacy of viscous flow solutions.

2) The three-dimensional flow features generated by finite-span wings present great challenges due to the effort required to visualize, measure, and compute the complex flows generated as a function of flapping mode, frequency, amplitude, wing geometry, and Reynolds number. Of special importance are the spanwise flow features which may include the formation and shedding of spanwise vortices. Still greater challenges are offered by the interactions between flapping wings in close proximity to each other.

3) Flapping-wing propulsion in nature involves flexible wings and the advantage of using flexible flapping wings for MAV applications

such as in Fig. 27 is demonstrated. However, the physics of the flow over flexible flapping wings is yet to be fully understood. Advances can be made through carefully designed experiments and the development of flow solvers that incorporate efficient and effective fluid-structure coupling.

4) One key application of studying flapping-wing aerodynamics is the determination of the conditions for optimal performance in terms of lift, thrust, and efficiency. Despite substantial research efforts as reviewed here, there is still a lack of full understanding of the physics governing the optimal aerodynamic performance of a flapping wing. Important parameters that influence the aerodynamics of a single flapping wing include the shape of the wing, the stiffness of the wing, the type of flapping motion (in terms of frequency, amplitude, and phase for pitch and plunge), and the Reynolds number. It is envisaged that state-of-the-art optimization techniques could be used not only to determine values of these parameters for optimal aerodynamic performance of flapping-wing propulsion but also to provide insight into the physics of flows for optimal performance of a flapping wing.

5) Modeling of transition from laminar to turbulent flows is very difficult even for fixed wing applications. Detailed experimental information is needed on the formation of separation bubbles. Although considerable progress has been made in this area for steady airfoil flows, very little is as yet known about the behavior of separation bubbles on oscillating airfoils. It is inevitable that advances in separation bubble formation and transition flow modeling are required before the benefits of flapping-wing propulsion can be fully exploited.

Clearly, the flapping-wing mechanisms that have evolved in nature present the aerodynamicist with many interesting and challenging problems requiring the computational and experimental investigation of highly complex and unsteady viscous and separated flows. Adoption or modification of these flapping-wing mechanisms is likely to lead to the development of new micro air vehicles that are capable of imitating the flight performance of birds and insects.

Acknowledgments

Max F. Platzer and Kevin D. Jones gratefully acknowledge the support of the Office of Naval Research, Naval Research Laboratory, and the Naval Postgraduate School Internal Research Program. Platzer is also grateful for the support of a UNSW@ADFA Rector Visiting Fellowship to undertake a portion of this investigation. Navier–Stokes calculations by J. Young and J. C. S. Lai were performed with the support of a grant under the Merit Allocation Scheme of the Australian Partnership for Advanced Computing National Facility (APAC-NF).

References

[1] Rozhdestvensky, K. V., and Ryzhov, V. A., "Aerohydrodynamics of Flapping-wing Propulsors," *Progress in Aerospace Sciences*, Vol. 39, No. 8, 2003, pp. 585–633. doi:10.1016/S0376-0421(03)00077-0

[2] Shyy, W., Berg, M., and Ljungqvist, D., "Flapping and Flexible Wings for Biological and Micro Air Vehicles," *Progress in Aerospace Sciences*, Vol. 35, No. 5, 1999, pp. 455–505. doi:10.1016/S0376-0421(98)00016-5

[3] Ho, S., Nassef, H., Pornsinsirirak, N., Tai, Y. C., and Ho, C. M., "Unsteady Aerodynamics and Flow Control for Flapping Wing Flyers," *Progress in Aerospace Sciences*, Vol. 39, No. 8, 2003, pp. 635–681. doi:10.1016/j.paerosci.2003.04.001

[4] Triantaflyllou, M. S., Techet, A. H., and Hover, F. S., "Review of Experimental Work in Biomimetic Foils," *IEEE Journal of Oceanic Engineering*, Vol. 29, No. 3, 2004, pp. 585–594. doi:10.1109/JOE.2004.833216

[5] Ansari, S. A., Zbikowski, R., and Knowles, K., "Aerodynamic Modelling of Insect-like Flapping Flight for Micro Air Vehicles," *Progress in Aerospace Sciences*, Vol. 42, No. 2, 2006, pp. 129–172. doi:10.1016/j.paerosci.2006.07.001

[6] Knoller, R., "Die Gesetze des Luftwiderstandes," *Flug- und Motortechnik (Wien)*, Vol. 3, No. 21, 1909, pp. 1–7.

[7] Betz, A., "Ein Beitrag zur Erklaerung des Segelfluges," *Zeitschrift fur Flugtechnik und Motorluftschiffahrt*, Vol. 3, 1912, pp. 269–272.

[8] Katzmayr, R., "Effect of Periodic Changes of Angle of Attack on Behavior of Airfoils," NACA TM 147, Oct. 1922.

[9] Taylor, G. K., Nudds, R. L., and Thomas, A. L. R., "Flying and Swimming Animals Cruise at a Strouhal Number Tuned for High Power Efficiency," *Nature (London)*, Vol. 425, Oct. 2003, pp. 707–711. doi:10.1038/nature02000

[10] Birnbaum, W., "Das ebene Problem des Schlagenden Fluegels," *Zeitschrift fuer Angewandte Mathematik und Mechanik*, Vol. 4, No. 4, Aug. 1924, pp. 277–292. doi:10.1002/zamm.19240040401

[11] von Kármán, T., and Burgers, J. M., "General Aerodynamic Theory—Perfect Fluids," *Aerodynamic Theory*, edited by W. F. Durand, Vol. 2, Julius Springer, Berlin, 1934, p. 308.

[12] Theodorsen, T., "General Theory of Aerodynamic Instability and the Mechanism of Flutter," NACA, Rept. 496, 1935.

[13] Garrick, I. E., "Propulsion of a Flapping and Oscillating Airfoil," NACA, Rept. 567, 1936.

[14] Teng, N. H., "The Development of a Computer Code for the Numerical Solution of Unsteady Inviscid and Incompressible Flow Over an Airfoil," M.S. Thesis, Naval Postgraduate School, Monterey, CA, June 1987.

[15] Cebeci, T., Platzer, M. F., Chen, S., Chang, K. C., and Shao, J. P., *Analysis of Low-Speed Unsteady Airfoil Flows*, Springer, New York, 2005.

[16] Jones, K. D., Lund, T. C., and Platzer, M. F., "Experimental and Computational Investigation of Flapping Wing Propulsion for Micro Air Vehicles," *Fixed and Flapping Wing Aerodynamics for Micro Air Vehicles*, Vol. 195, Progress in Astronautics and Aeronautics, AIAA, New York, 2001, pp. 307–339, Chap. 16.

[17] Lewin, G. C., and Haj-Hariri, H., "Modelling Thrust Generation of a Two-Dimensional Heaving Airfoil in a Viscous Flow," *Journal of Fluid Mechanics*, Vol. 492, 2003, pp. 339–362. doi:10.1017/S0022112003005743

[18] Young, J., "Numerical Simulation of the Unsteady Aerodynamics of Flapping Airfoils," Ph.D. Thesis, The University of New South Wales, at the Australian Defence Force Academy, May 2005.

[19] Young, J., and Lai, J. C. S., "Vortex Lock-in Phenomenon in the Wake of a Plunging Airfoil," *AIAA Journal*, Vol. 45, No. 2, 2007, pp. 485–490. doi:10.2514/1.23594

[20] Lai, J. C. S., and Platzer, M. F., "Jet Characteristics of a Plunging Airfoil," *AIAA Journal*, Vol. 37, No. 12, 1999, pp. 1529–1537.

[21] Bratt, J. B., *Flow Patterns in the Wake of an Oscillating Airfoil*, Aeronautical Research Council, 1953, pp. 17–24.

[22] Jones, K. D., Dohring, C. M., and Platzer, M. F., "Experimental and Computational Investigation of the Knoller-Betz Effect," *AIAA Journal*, Vol. 36, No. 7, July 1998, pp. 1240–1246.

[23] Tuncer, I. H., Walz, R., and Platzer, M. F., "A Computational Study of the Dynamic Stall of a Flapping Airfoil," AIAA Paper 98-2519, June 1998.

[24] Young, J., and Lai, J. C. S., "Oscillation Frequency and Amplitude Effects on the Wake of a Plunging Airfoil," *AIAA Journal*, Vol. 42, No. 10, 2004, pp. 2042–2052.

[25] Young, J., and Lai, J. C. S., "Mechanisms Influencing the Efficiency of Oscillating Airfoil Propulsion," *AIAA Journal*, Vol. 45, No. 7, July 2007, pp. 1695–1702. doi:10.2514/1.27628

[26] Heathcote, S., Wang, Z., and Gursul, I., "Effect of Spanwise Flexibility on Flapping Wing Propulsion," *Journal of Fluids and Structures*, Vol. 24, No. 2, 2008, pp. 183–199. doi:10.1016/j.jfluidstructs.2007.08.003

[27] Lua, K. B., Lim, T. T., Yeo, K. S., and Oo, G. Y., "Wake-Structure Formation of a Heaving Two-Dimensional Elliptic Airfoil," *AIAA Journal*, Vol. 45, No. 7, July 2007, pp. 1571–1583. doi:10.2514/1.25310

[28] Koochesfahani, M. M., "Vortical Patterns in the Wake of an Oscillating Airfoil," *AIAA Journal*, Vol. 27, No. 9, 1989, pp. 1200–1205.

[29] Anderson, J. M., Streitlin, K., Barrett, D. S., and Triantafyllou, M. S., "Oscillating Foils of High Propulsive Efficiency," *Journal of Fluid Mechanics*, Vol. 360, 1998, pp. 41–72. doi:10.1017/S0022112097008392

[30] Isogai, K., Shinmoto, Y., and Watanabe, Y., "Effects of Dynamic Stall on Propulsive Efficiency and Thrust of Flapping Airfoil," *AIAA Journal*, Vol. 37, No. 10, Oct. 1999, pp. 1145–1151.

[31] Tuncer, I. H., and Platzer, M. F., "Computational Study of Flapping Airfoil Aerodynamics," *Journal of Aircraft*, Vol. 37, No. 3, May–June 2000, pp. 514–520.

[32] Ramamurti, R., and Sandberg, W., "Simulation of Flow about Flapping Airfoils Using Finite Element Incompressible Flow Solver," *AIAA Journal*, Vol. 39, No. 2, Feb. 2001, pp. 253–260.

[33] Guglielmini, L., and Blondeaux, P., "Propulsive Efficiency of Oscillating Foils," *European Journal of Mechanics B Fluids*, Vol. 23, No. 2, 2004, pp. 255–278. doi:10.1016/j.euromechflu.2003.10.002

[34] Tuncer, I. H., and Kaya, M., "Optimization of Flapping Airfoils for Maximum Thrust and Propulsion Efficiency," *AIAA Journal*, Vol. 43, No. 11, Nov. 2005, pp. 2329–2341.

[35] Lian, Y., and Shyy, W., "Laminar-Turbulent Transition of a Low Reynolds Number Rigid or Flexible Airfoil," AIAA Paper 2006-3051, June 5–8, 2006.

[36] Heathcote, S., and Gursul, I., "Flexible Flapping Airfoil Propulsion at Low Reynolds Numbers," *AIAA Journal*, Vol. 45, No. 5, May 2007, pp. 1066–1079. doi:10.2514/1.25431

[37] Neef, M. F., and Hummel, D., "Euler Solutions for a Finite-Span Flapping Wing," *Progress in Astronautics and Aeronautics*, Vol. 195, 2001, Chap. 19, pp. 429–451.

[38] Hall, K. C., and Hall, S. R., "A Rational Engineering Analysis of the Efficiency of Flapping Flight," *Progress in Astronautics and Aeronautics*, Vol. 195, 2001, Chap. 13, pp. 249–274.

[39] von Ellenrieder, K. D., Parker, K., and Soria, J., "Flow Structure behind a Heaving and Pitching Finite-Span Wing," *Journal of Fluid Mechanics*, Vol. 490, Sept. 2003, pp. 129–138. doi:10.1017/S0022112003005408

[40] Blondeaux, P., Fornarelli, F., Guglielmini, L., Triantafyllou, M. S., and Verzicco, R., "Numerical Experiments on Flapping Foils Mimicking Fish-like Locomotion," *Physics of Fluids*, Vol. 17, 2005, pp. 113601-1 to 12.

[41] Parker, K., von Ellenrieder, K. D., Soria, J., "Using Stereo Multigrid DPIV (SMDPIV) Measurements to Investigate the Vertical Skeleton Behind a Finite-Span Flapping Wing," *Experiments in Fluids*, Vol. 39, No. 2, Aug. 2005, pp. 281–298. doi:10.1007/s00348-005-0971-y

[42] Spentzos, A., Barakos, G. N., Badcock, K. J., Richards, B. E., Coton, F. N., Galbraith, R. A. McD., Berton, E., and Favier, D., "Computational Fluid Dynamics Study of Three-Dimensional Dynamic Stall of Various Planform Shapes," *Journal of Aircraft*, Vol. 44, No. 4, 2007, pp. 1118–1128. doi:10.2514/1.24331

[43] Lai, J. C. S., and Platzer, M. F., "Characteristics of a Plunging Airfoil at Zero Freestream Velocity," *AIAA Journal*, Vol. 39, No. 3, 2001, pp. 531–534.

[44] Heathcote, S., Martin, D., and Gursul, I., "Flexible Flapping Airfoil Propulsion at Zero Freestream Velocity," *AIAA Journal*, Vol. 42, No. 11, Nov. 2004, pp. 2196–2204.

[45] Freymuth, P., "Thrust Generation by an Airfoil in Hover Modes," *Experiments in Fluids*, Vol. 9, No. 1, 1990, pp. 17–24. doi:10.1007/BF00575331

[46] Sunada, S., Kawachi, K., Matsumoto, A., and Sakaguchi, A., "Unsteady Forces on a Two-Dimensional Wing in Plunging and Pitching Motions," *AIAA Journal*, Vol. 39, No. 7, 2001, pp. 1230–1239.

[47] Ellington, C. P., and Usherwood, J. R., "Lift and Drag Characteristics of Rotary and Flapping Wings," *Progress in Astronautics and Aeronautics*, Vol. 195, 2001, Chap. 12, pp. 231–248.

[48] Dickinson, M. H., and Goetz, K. G., "Unsteady Aerodynamic Performance of Model Wings at Low Reynolds Numbers," *Journal of Experimental Biology*, Vol. 174, 1993, pp. 45–64.

[49] Dickinson, M. H., "The Effects of Wing Rotation on Unsteady Aerodynamic Performance at Low Reynolds Numbers," *Journal of Experimental Biology*, Vol. 192, 1994, pp. 179–206.

[50] Sane, S. P., and Dickinson, M. H., "The Control of Flight Force by a Flapping Wing: Lift and Drag Production," *Journal of Experimental Biology*, Vol. 204, No. 15, 2001, pp. 2607–2626.

[51] Zbikowski, R., "On Aerodynamic Modelling of an Insect-like Flapping Wing in Hover for Micro Air Vehicles," *Philosophical Transactions of the Royal Society of London, Series A: Mathematical and Physical Sciences*, Vol. 360, No. 1791, 2002, pp. 273–290. doi:10.1098/rsta.2001.0930

[52] Ansari, S. A., Zbikowski, R., and Knowles, K., "Nonlinear Unsteady Aerodynamic Model for Insect-like Flapping Wings in the Hover Part 1: Methodology and Analysis," *Proceedings of the Institute of Mechanical Engineering, Part G: Journal of Aerospace Engineering*, Vol. 220, No. 2, April 2006, pp. 61–83; also "Nonlinear Unsteady Aerodynamic Model for Insect-like Flapping Wings in the Hover Part 2: Implementation and Validation," *Proceedings of the Institute of Mechanical Engineering, Part G: Journal of Aerospace Engineering*, Vol. 220, No. 3, June 2006, pp. 169–186.

[53] Kurtulus, D. F., Farcy, A., and Alemdaroglu, N., "Unsteady Aerodynamics of Flapping Airfoil in Hovering Flight at Low Reynolds Numbers," AIAA Paper 2005-1356, Jan. 2005.

[54] Kurtulus, D. F., David, L., Farcy, A., and Alemdaroglu, N., "Aerodynamic Characteristics of Flapping Motion in Hover," *Experiments in Fluids*, Vol. 44, No. 1, 2008 pp. 23–36. doi:10.1007/s00348-007-0369-0

[55] Liu, H., Ellington, C. P., Kawachi, K., Van Den Berg, C., and Willmott, A. P., "A Computational Fluid Dynamic Study of Hawk-Moth Hovering," *Journal of Experimental Biology*, Vol. 201, 1998, pp. 461–477.

[56] Liu, H., and Kawachi, K., "Leading-Edge Vortices of Flapping and Rotary Wings at Low Reynolds Number," *Progress in Astronautics and Aeronautics*, Vol. 195, 2001, Chap. 14, pp. 275–285.

[57] Liu, H., "Computational Biological Fluid Dynamics: Digitizing and Visualizing Animal Swimming and Flying," *Integrative and Comparative Biology*, Vol. 42, No. 5, 2002, pp. 1050–1059. doi:10.1093/icb/42.5.1050

[58] Ramamurti, R., and Sandberg, W. C., "Computational Study of 3-D Flapping Foil Flows," AIAA Paper 2001-0605, Jan. 2001.

[59] Dickinson, M. H., Lehmann, F. O., and Sane, S., "Wing Rotation and the Aerodynamic Basis of Insect Flight," *Science*, Vol. 284, No. 5422, 1999, pp. 1954–1960. doi:10.1126/science.284.5422.1954

[60] Young, J., Lai, J. C. S., and Germain, C., "Numerical Simulation and Parameter Variation of Insect Wing Motion based on Dragonfly Hovering," *AIAA Journal*, (to be published).

[61] Wootton, R. J., and Kukalova-Peck, J., "Flight Adaptations in Palaeozoic Palaeoptera," *Biological Reviews of the Cambridge Philosophical Society*, Vol. 75, No. 1, 2000, pp. 129–167.

[62] Bosch, H., *Interfering Airfoils in Two-Dimensional Unsteady Incompressible Flow*, CP-277, AGARD, Paper 7, Sept. 1977.

[63] Lan, C. E., "The Unsteady Quasi-Vortex-Lattice Method with Application to Animal Propulsion," *Journal of Fluid Mechanics*, Vol. 93, No. 4, 1979, pp. 747–765. doi:10.1017/S0022112079002019

[64] Schmidt, W., "Der Wellpropeller, ein Neuer Antrieb fuer Wasser-, Land-, und Luftfahrzeuge," *Zeitschrift fur Flugwissenschaften*, Vol. 13, 1965, pp. 427–479.

[65] Platzer, M. F., Neace, K. S., and Pang, K. C., "Aerodynamic Analysis of Flapping Wing Propulsion," AIAA Paper 93-0484, Jan. 1993.

[66] Tuncer, I. H., and Platzer, M. F., "Thrust Generation Due to Airfoil Flapping," *AIAA Journal*, Vol. 34, No. 2, Feb. 1996, pp. 324–331.

[67] Jones, K. D., and Platzer, M. F., "Time-Domain Analysis of Low-Speed Airfoil Flutter," *AIAA Journal*, Vol. 34, No. 5, May 1996, pp. 1027–1033.

[68] Zhu, Q., Wolfgang, M. J., Yue, D. K. P., and Triantafyllou, M. S., "Three-Dimensional Flow Structures and Vorticity Control in Fish-like Swimming," *Journal of Fluid Mechanics*, Vol. 468, 2002, pp. 1–28. doi:10.1017/S002211200200143X

[69] Jones, K. D., Castro, B. M., Mahmoud, O., and Platzer, M. F., "A Numerical and Experimental Investigation of Flapping Wing Propulsion in Ground Effect," AIAA Paper 2002-0866, Jan. 2002.

[70] Tuncer, I. H., and Kaya, M., "Thrust Generation Due to Flapping Airfoils in a Biplane Configuration," *Journal of Aircraft*, Vol. 40, No. 3, May–June 2003, pp. 509–515.

[71] Jones, K. D., Bradshaw, C. J., Papadopoulos, J., and Platzer, M. F., "Bio-Inspired Design of Flapping-Wing Micro Air Vehicles," *The Aeronautical Journal*, Vol. 109, No. 1098, Aug. 2005, pp. 385–393.

[72] Norberg, R. A., "Hovering Flight of the Dragonfly Aeschna Juncea: Kinematics and Aerodynamics," *Swimming and Flying in Nature*, Plenum Press, New York, 1975.

[73] Saharon, D., and Luttges, M., "Three-Dimensional Flow Produced by a Pitching-Plunging Model Dragonfly Wing," AIAA Paper 87-0121, Jan. 1987.

[74] Saharon, D., and Luttges, M., "Visualization of Unsteady Separated Flow Produced by Mechanically Driven Dragonfly Wing Kinematics Model," AIAA Paper 88-0569, Jan. 1988.

[75] Saharon, D., and Luttges, M., "Dragonfly Unsteady Aerodynamic: The Role of the Wing Phase Relations in Controlling the Produced Flows," AIAA Paper 89-0832, Jan. 1989.

[76] Isogai, K., and Shinmoto, Y., "Study on Aerodynamic Mechanism of Hovering Insects," AIAA Paper 2001-2470, June 2001.

[77] Kim, D., and Choi, H., "Vortical Motion Caused by Two Flapping Wings," *2nd International Symposium Aqua-Bio-Mechanisms*, Tokai University, Honolulu, Hawaii, Sept. 2004.

[78] Isogai, K., Fujishoro, S., Saitoh, T., Yamamoto, M., Yamasaki, M., and Matsubara, M., "Unsteady Three-Dimensional Viscous Flow Simulation of a Dragonfly Hovering," *AIAA Journal*, Vol. 42, No. 10, Oct. 2004, pp. 2053–2059.

[79] Kornbluh, R. D., Low, T. P., Stanford, S. E., Vinande, E., Bonwit, N., Holeman, D., DeLaurier, J. D., Loewen, D., Zdunich, P., MacMaster, M., and Bilyk, D., "Flapping-wing Propulsion Using Electroactive Polymer Artificial Muscle Actuators, Phase 2: Radio-controlled Flapping-wing Testbed," SRI International, Rept. ITAD-3470-FR-03-009, 2002.

[80] Ramamurti, R., Sandberg, W., Valana, P., Kellogg, J., and Cylinder, D., "Computational Fluid Dynamics Study of Unconventional Air Vehicle Configurations," *The Aeronautical Journal*, Vol. 109, No. 7, July 2005, pp. 337–347.

[81] Arina, R., Atkin, C., Hanff, E., Jones, K. D., Lekas, T., Ol, M., Khalid, M., McAuliffe, B., Paquet, J. B., Platzer, M., Radespiel, R., Rist, U., Windte, J., and Yuan, W., "Experimental and Computational Investigations in Low Reynolds Number Aerodynamics, with Applications to Micro Air Vehicles," NATO-RTO, TR. AVT-101, 2006.

G. Abate
Guest Editor